ACADEMIA ROMÂNĂ
Revue Roumaine de Chimie
http://web.icf.ro/rrch/

Rev. Roum. Chim.,
2018, *63*(12), 1135-1147

ADSORPTION OF *p*-NITROPHENOL ON ACTIVATED CARBON DERIVED FROM THE LIGNIN OF CELLULOSIC ETHANOL BY-PRODUCT

Zhe ZHAO,[a] Xiaofeng GOU,[a] Shuqi FANG,[a,b] Chun CHANG,[a,b] Hongping LI [a] and Xiuli HAN[a,b*]

[a]School of Chemical Engineering and Energy, Zhengzhou University, Kexue Road 100#, Zhengzhou, Henan 450001(China)
[b]Engineering Laboratory of Henan Province for Biorefinery Technology and Equipment,
Kexue Road 100#, Zhengzhou, Henan 450001(China)

Received January 22, 2018

Adsorption of *p*-nitrophenol (PNP) onto activated carbon (AC) prepared from lignin of cellulosic ethanol by-product has been experimented. Effects of contact time, AC dosage, pH, initial PNP concentration and temperature were investigated using batch experiments. Isotherm models such as Langmuir, Freundlich, Temkin and Redlich-Peterson were employed to evaluate the PNP adsorption behavior. The results indicated that Langmuir isotherm can well describe the PNP adsorption process and the maximum monolayer adsorption capacity was 1.03 mmol/g at 298 K. The PNP adsorption process followed the pseudo-first-order, suggesting that the PNP adsorption on AC may be a physical adsorption process. Brunauer-Emmett-Teller, Scanning electron microscopy, Fourier transform infrared spectroscopy and thermogravimetry were used to analyze the characteristics of AC. Adsorption mechanism was discussed, and it is clear that adsorption process was influenced by the H-bonding, π-π interaction and electrostatic repulsion. It showed that AC derived from the lignin of cellulosic ethanol by-product was an excellent adsorbent for PNP removal.

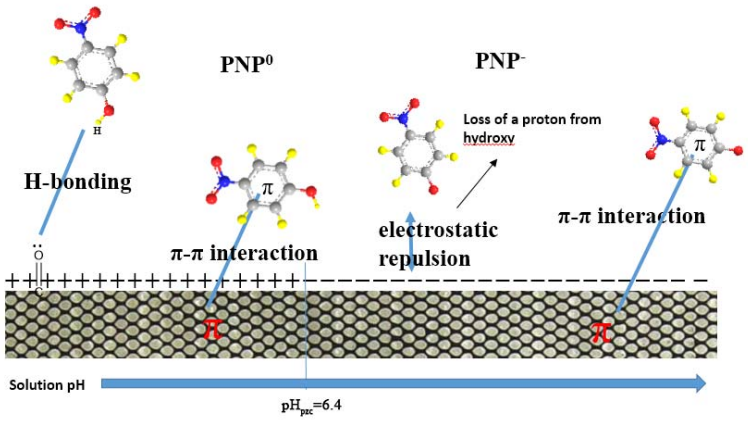

INTRODUCTION

Nowadays, the surface water and even ground water were contaminated due to the widely use of chemicals, such as dye,[1] antibiotics,[2] and nitroaromatic compound[3] *et al.*. PNP, one kind of nitroaromatic compound, was largely used in manufacturing pesticides, explosives and dyestuffs,[3] and the PNP wastewater can be discharged into the environment system. The presence of PNP in the aquatic environment has received considerable attention in recent years. It is known that PNP is hazard to organisms owing to its persistent, bio-accumulative and toxic even at low concentration. The US Environmental Protection Agency (EPA) has selected PNP as one of 126 priority pollutants.[4] Therefore, wastewaters containing *p*-nitrophenol should be specifically treated.

Recently, different water treatment methods, including adsorption,[5] chemical oxidation,[6] advanced oxidation process,[7,8] extraction[9] and biodegradation[10] have been researched to treat wastewater. Among these technologies, adsorption method is usually selected because of its features

* Corresponding author: xlhan@zzu.edu.cn; Tel: +86 371 67780093, Fax: +86 371 67780093

of simple-design, high-efficiency and easy-operation.[11,12] AC has been one of the widely used adsorbents due to its easy disposal, and environment-friendly.[13] AC was usually produced by coal in industrial process.[14] However, coal is non-renewable fossil oil resource, so the way to replace the coal by the natural, renewable and low-cost materials is beneficial.[15]

A strong global interest in renewable bioethanol derived from cellulosic biomass is drove by the concern about the exhaustion of nonrenewable fossil fuel resources.[16] Currently, the cellulose biorefining technology is in the fleet developing stage.[17] Cellulosic biomass, such as crops straw, contains lots of cellulose, hemicellulose and lignin. In biorefining process, cellulose and hemicellulose are transformed into ethanol, while the unavailable lignin is left behind as solid residue. If this lignin can get effective use, it will greatly reduce the cost of cellulosic ethanol production. Therefore, how to use the lignin of cellulosic ethanol by-product has become a research hotspot at home and abroad.

Due to its abundance, low-cost and high carbon content, lignin seems to be an adequate material for the preparation of AC.[18] In this research, lignin of cellulosic ethanol by-product was used to produce AC. Adsorption characteristics of PNP onto AC prepared from lignin of cellulosic ethanol by-product were also investigated.

MATERIALS AND METHODS

Materials

AC was produced from lignin of cellulosic ethanol by-product, obtained from the Henan Tianguan Group Co., Ltd., Nanyang City, by the steam activation technology. Lignin was put into a pyrolysis furnace at 400 °C without air; a char called carbonized lignin was left. In the activation step, 10 g of carbonized lignin was heated in a quartz tube under N_2 flow from room temperature to necessary activation temperature 889 °C with the heating rate of 10 °C/min. Flowing steam rapidly replaced nitrogen flow when activation temperature was reached, then keeping at this temperature for 26 min. Finally, steam was switched to nitrogen flowing until the product was cooled to room temperature.[19]

Materials characterization

AC prepared from lignin of cellulosic ethanol by-product was analyzed for its characteristics using Brunauer-Emmett-Teller (BET; Quantachrome Instrument, USA), Fourier transform infrared spectroscopy (FTIR; PE-1710, USA), scanning electron microscopy (SEM; JEOL 6335F-SEM, Japan) and thermogravimetric analysis(TG; TA 2000, USA). A solid addition method was used to obtain the point of zero charge(pH_{pzc}) of AC.[20]

Preparation of PNP solution

PNP (≥99%, $C_6H_5NO_3$, FW=139.11) was supplied by Shanghai Chemical Dispensing Factory of Shanghai Municipality, China. Stock solution (5 mmol/L) was obtained by dissolving 5 mmol PNP in a 1 L volumetric flask with distilled water. Experiment solutions of PNP were gained by diluting the stock solutions with distilled water and the pH was adjusted with 0.1 mol/L HCl solutions or 0.1mol/L NaOH solutions.

Adsorption experiments

In adsorption experiment, the various adsorption parameters such as reaction time, pH, initial PNP concentration and temperature were all evaluated. The 0.02 g AC were mixed with 20 mL PNP solution of the desired concentration and the desired pH in a 50 mL conical flask, then shaken by a water bath shaker agitating at 100 rpm. After adsorption, the AC in solutions was extracted using the centrifugation technology and the PNP concentrations of the remnant solutions were determined by an UV-vis spectrophotometer (UV-755B) at the wavelength of 317 nm. The adsorption kinetic experiments were implemented by analyzing the adsorptive uptake of PNP of certain concentrations from 0.5 - 1.5 mmol/L or certain temperature from 298 - 318 K at different time intervals. PNP solutions of different concentrations (0.2 - 1.6 mmol/L) were shaken with a certain amount of AC at 298, 308 and 318 K till reached the equilibrium in order to study the adsorption isotherm.

The amount of PNP adsorbed on AC was calculated by Equation (1):

$$q_e = \frac{V(C_0 - C_e)}{m} \quad (1)$$

where q_e (mmol/g) was the amount of PNP adsorbed on AC at the time of equilibrium; V (L) was the solution volume; m (g) was the mass of AC; C_0 (mmol/L) and C_e (mmol/L) were the initial and equilibrium concentrations of PNP, respectively.

ADSOTPTION MODELS

Adsorption kinetic models

Adsorption kinetics are vital in investigating the controlling mechanism in PNP adsorption process. The pseudo-first-order, pseudo-second-order, Elovich and the intraparticle diffusion model were applied to fit the adsorption kinetics data. Those equations of kinetic models are as follows, respectively:
Pseudo-first-order model:

$$q_t = q_e(1-e^{-k_1 t}) \tag{2}$$

Pseudo-second-order model:

$$q_t = \frac{k_2 q_e^2 t}{1+k_2 q_e t} \tag{3}$$

Elovich model:

$$q_t = \frac{1}{\beta}\ln(\alpha\beta)+\frac{1}{\beta}\ln t \tag{4}$$

Intra-particle diffusion model:

$$q_t = k_{ti} t^{0.5} + C \tag{5}$$

where k_1 (1/min) and k_2 (g/(mmol min)) were the pseudo-first-order and pseudo-second-order kinetic adsorption rate constant, respectively; q_t (mmol/g) represented the adsorption capacity of AC at any instant of time; q_e (mmol/g) represented the equilibrium adsorption capacity; t (min) represented the contact time; α is the initial adsorption rate (mmol/(g min)); β is the adsorption constant (g/mmol); C was the constant; k_{ti} (mmol/(g $\text{min}^{1/2}$)) was the intraparticle diffusion rate constant.

Adsorption equilibrium models

Adsorption equilibriums are significant for the study of PNP adsorption system. Isotherm models, such as Langmuir, Freundlich, Temkin and Redlich-Peterson were applied to explain the experimental data.
Langmuir:

$$q_e = \frac{q_m K_L C_e}{1+K_L C_e} \tag{6}$$

Freundlich:

$$q_e = K_F C_e^{1/n} \tag{7}$$

Temkin:

$$q_e = A + B\ln C_e = \frac{RT}{b_t}\ln a_t + \frac{RT}{b_t}\ln C_e \tag{8}$$

Redlich-Peterson:

$$q_e = \frac{AC_e}{1+BC_e^g} \tag{9}$$

where q_e (mmol/g) was the PNP equilibrium adsorption capacity; q_m (mmol/g) was the saturation adsorption capacity; K_L (L/mmol) was the Langmuir constant; K_F (mmol/(g $(\text{mmol/L})^{1/n}$)) was the Freundlich adsorption constant; C_e (mmol/L) was the PNP equilibration concentration; The parameter n was the empirical constant, and value of n was an indication of the favorability of adsorption; a_t and b_t were the Temkin model parameter; A (L/g) and B (L/mmol) were the Redlich-Peterson model constant; The g was a constant fluctuated between 0 and 1 with two specific behaviors: Langmuir form for g = 1 and Henry's law form for g = 0.

RESULTS AND DISCUSSION

The characterization of absorbent

The BET surface area and porous properties of AC derived from lignin of cellulosic ethanol by-product were determined from N_2 adsorption experiments. Microporous surface and micropore volume, as well as external surface were evaluated by t-plot method. $D_p=4V_{total}/S_{BET}$ was used to calculate the average pore width, V_T was the total volume of pores, and S represented the BET surface area.

Fig. 1 shows the typical nitrogen adsorption–desorption isotherms and the pore size distribution of the AC. As shown in Fig. 1, a sharp increase in N_2 adsorption appeared when P/P_0 was low, suggesting that the AC possesses micropores. There, the S_{BET} of the AC was estimated to be 313.21 m^2/g, total pore volume was 0.2828 cm^3/g. Micropore area and micropore volume of AC were 207.33 m^2/g and 0.0860 cm^3/g according to the t-plot method. Average pore width of AC was 3.98 nm.

Fig. 2 shows the morphological characteristic of the carbonized lignin and AC using SEM technology. It is clearly that AC had an irregular and porous external surface with lots of cavities, cracks and irregular protrusions. This extraordinary structure greatly improved the PNP adsorption capacity of material.

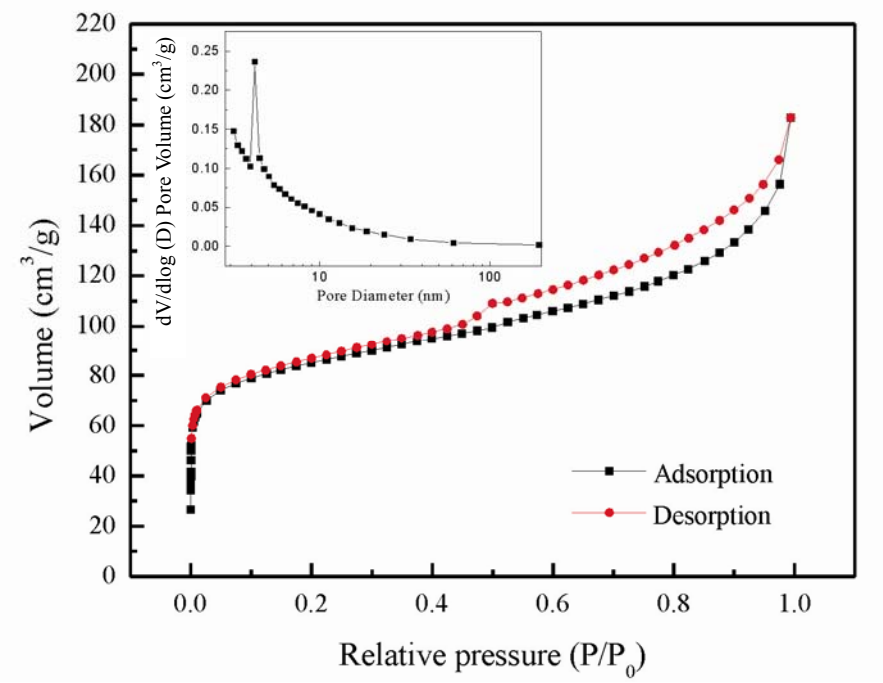

Fig. 1 – Nitrogen adsorption/desorption isotherms and pore size distribution of AC.

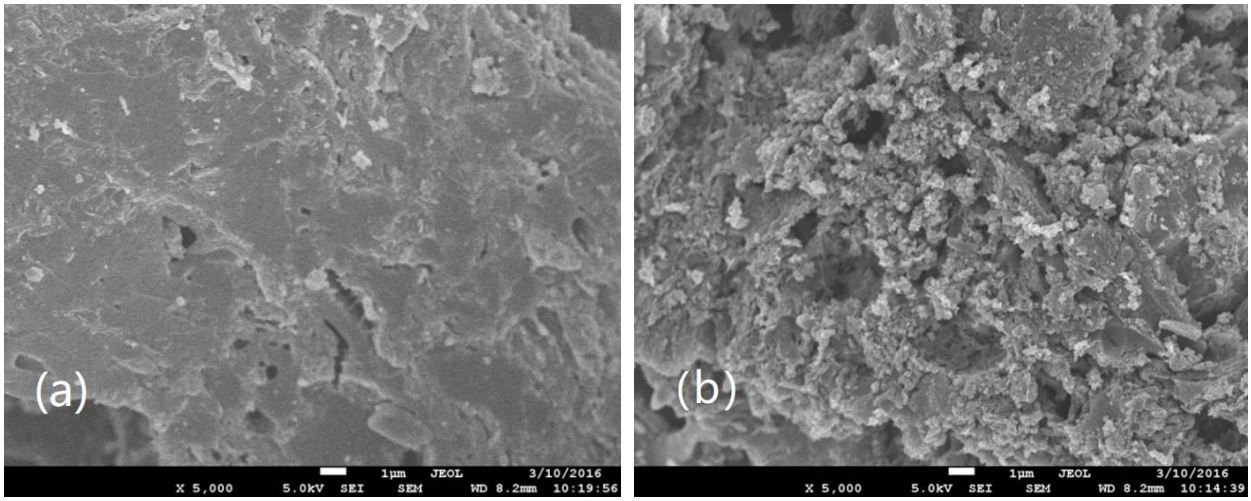

Fig. 2 – The SEM images of carbonized lignin (a) and AC (b).

FTIR spectroscopy was used to determine the primary functional groups of the PNP and AC derived from lignin of cellulosic ethanol by-product before and after PNP adsorption(Fig. 3). The FTIR spectra of PNP and AC with and without PNP were performed using the KBr disc method in the scanning range of 4000-400 cm^{-1}. The infrared spectrum of PNP(Fig. 3a) is characterized by band at 3330.18 cm^{-1} assigned to O-H stretching vibration of the phenol unit. The bands at 1592.76 and 1502.09 cm^{-1} can be assigned to bending modes of aromatic rings in PNP. The band at 849.52 cm^{-1} is attributed to the out-of-plane bending vibration of =C-H on the benzene ring with the para substituents, such as $-NO_2$ and -OH. Band at 1324.58 cm^{-1} indicates the symmetrical stretching vibration of $Ar-NO_2$. The various bands representing structure of the AC before PNP adsorption experiment were displayed in Fig. 3b. The FTIR spectrum of AC showed a broad band at 3441.58 cm^{-1}, which was ascribable to the stretching vibration of O-H bands in hydroxyl functional groups or adsorbed water. The band at 1628.39 cm^{-1} represented the C=O group stretching. An obvious band at 1082.03 cm^{-1} implied the stretching vibrations of C-O. The spectral profile of the AC with adsorbed PNP shows differences from that of the AC due to the adsorbed PNP. It is observed from Fig. 3c that there was slight shift in position and changes in intensity of the bands after PNP adsorption experiment. These bands are observed in the infrared

spectrum of the AC with adsorbed PNP at 850.87, 1333.91, 1510.37 and 1593.46 cm^{-1}. These changes in FTIR spectroscopy demonstrate that PNP was adsorbed on activated carbon successfully.

Thermogravimetric analyses of the AC with and without PNP were obtained by using thermal analyzer(TA 2000) under an N_2 atmosphere from room temperature to 800 °C at a heating rate of 10 °C/min. Thermogravimetric(TG) and derivative thermogravimetric(DTG) curves demonstrate weight loss changing with an elevated temperature, as shown in Fig. 4. As seen from the TG-DTG curves for AC in Fig. 4, there is always a evident peak below 100 °C which can be explained by the loss of the dissociative or adsorbed water molecules within the AC particles. On the other hand, the AC derived from the lignin of cellulosic ethanol by-product exhibited high thermal stability, presenting residual mass of 90.6% at 800°C, indicating a complete degradation of lignocellulosic materials during the carbonization and activation procedures. The mass loss was observed from the TG-DTG curves of PNP adsorbed on AC, where PNP adsorption resulted in slightly lower temperature observed for the dehydration (< 50°C and 72°C).[1] The mass loss peak at 283°C may be attributed to the removal and desorption of PNP from the AC.

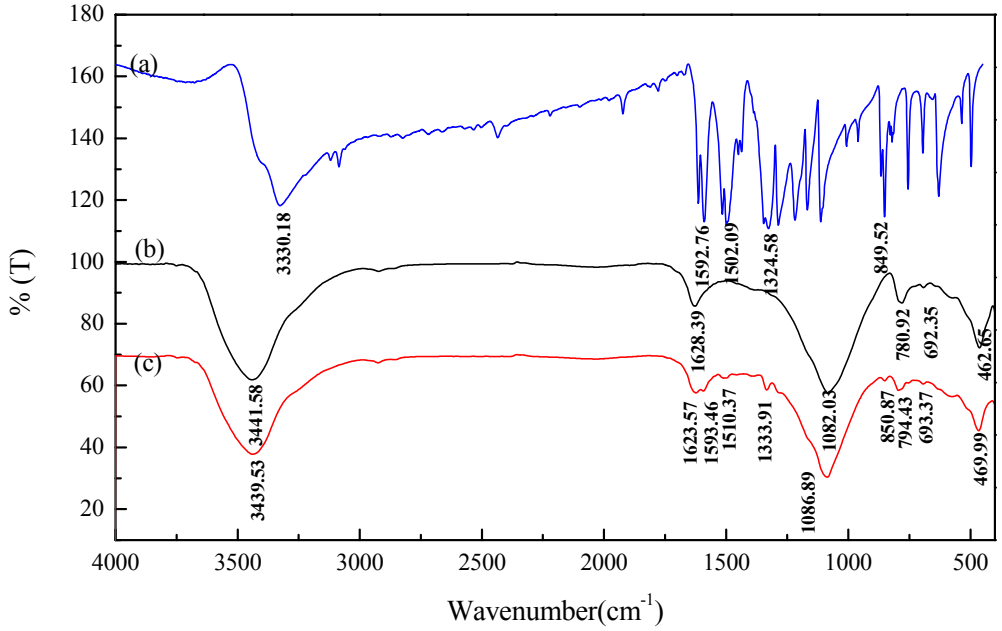

Fig. 3 – FTIR spectra of PNP(a), activated carbon(b) and activated carbon with adsorbed PNP (c).

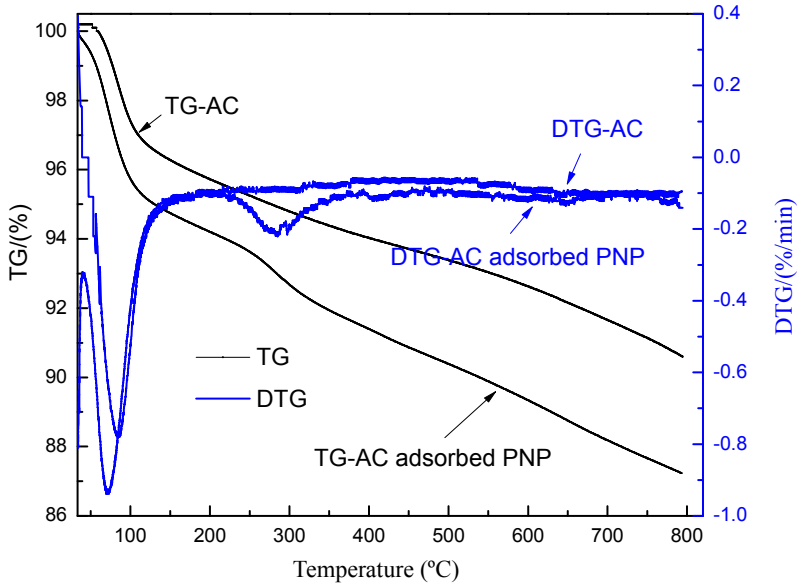

Fig. 4 – TG-DTG curves of AC before and after PNP adsorption.

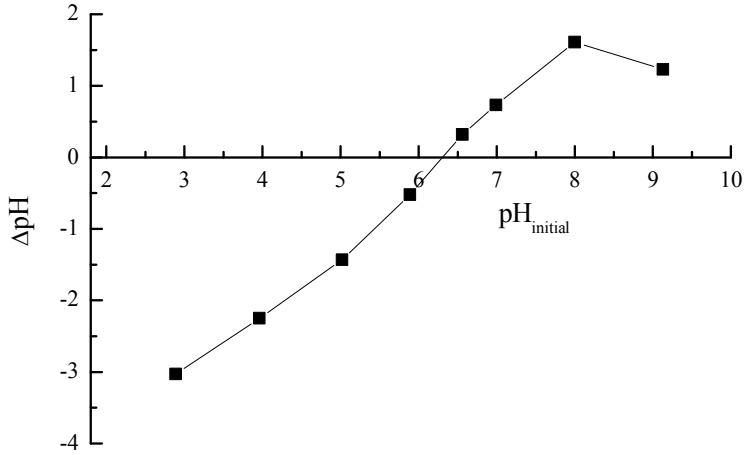

Fig. 5 – The point of zero charge of AC.

The point of zero charge(pH_{pzc}) of AC derived from lignin of cellulosic ethanol by-product was determined using a method proposed by Rivera-Utrilla *et al*.[20] Portions of 20 mL of 0.01 mol/L NaCl solution were placed in different conical flasks. The pH was adjusted to a value between 2 and 10 by addition of 0.1 mol/L NaOH or 0.1 mol/L HCl solutions. The AC sample(0.02 g) was added to each conical flask, and then shaken for 6 h to reach equilibrium. The pH of the initial solution and final solution designated as $pH_{initial}$ and pH_{final}, respectively. The pH at which the curve ΔpH (ΔpH= $pH_{initial}$-pH_{final}) vs. $pH_{initial}$ crossed the abscissa was taken as the $pH_{pzc.}$ As shown in Fig. 5, the pH_{pzc} of the AC was around 6.4. When the solution pH was below the pH_{pzc}, the surface charge of AC was positive. On the other hand, when the solution pH was above the pH_{pzc}, the surface charge of the AC was negative.

Effect of contact time

Contact time is an essential factor influencing adsorption of PNP on AC. There, 1 mmol/L PNP solution was used as the experiment object. Fig. 6 shows the effect of time on the PNP adsorption capacity of AC. The PNP adsorption capacity of AC increased fleetly for an initial short time. In this step, there were a large number of available active binding sites on the surface of AC, thus causing the initial PNP high adsorption rate. After some time, the PNP adsorption rate become slower, which may be explained by the decreasing of the available binding sites on the surface of AC. Fig. 6 shows that the adsorption of PNP reached equilibrium in 60 min. Other research selected 60 min as the experiment time to ensure the PNP adsorption equilibrium.

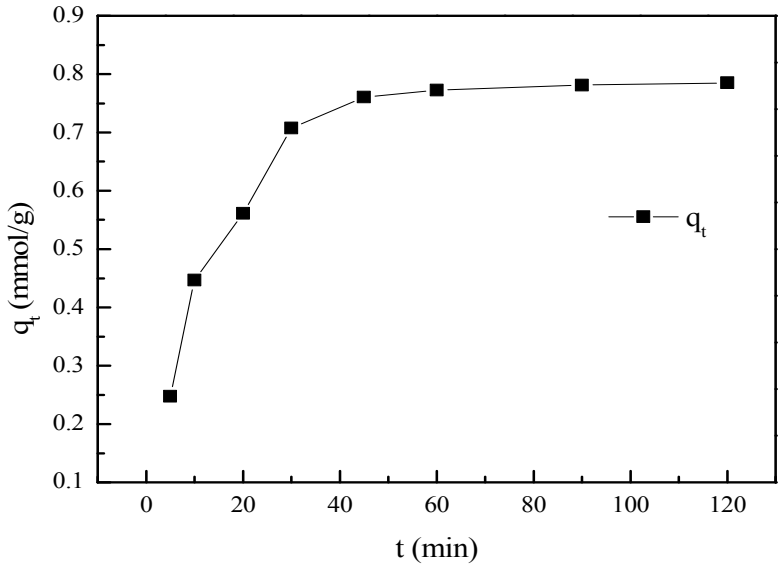

Fig. 6 – Effect of contact time on the adsorption capacity of AC(C_0=1.0 mmol/L; adsorbent concentration=1g/L; initial pH=6.57; T=298K).

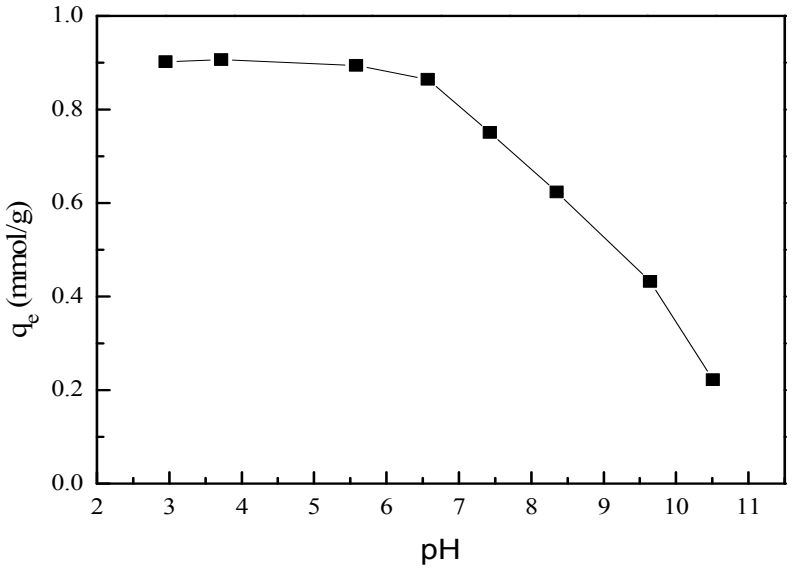

Fig. 7 – Effect of pH on the adsorption capacity of PNP (C_0=1.0 mmol/L; adsorbent concentration=0.5g/L; t=60min; T=298K).

Effect of solution pH

The pH of PNP solution has significant effect on the adsorption process. Effect of the pH on the adsorption capacity of AC was researched over a pH range 2.95 - 10.51 with PNP concentration of 1 mmol/L (Fig. 7). As initial pH of PNP solution increased from 2.95 to 6.57, adsorption capacity of AC only had a slight change. But when pH increased to higher than 6.57, the adsorption amount of PNP sharply decreased, especially at alkaline condition. So the low pH was helpful for the adsorption of PNP onto AC.

The distribution coefficient[22] of *p*-nitrophenol was shown in Fig. 8. The pKa value for PNP's acid dissociation constants is 7.15, so it can exist as molecule form PNP^0 and anionic form PNP^- as a function of pH.[23] When pH < 6, molecule form PNP^0 became the primary species. At pH=7.15, 50% molecule form PNP^0 has become anionic form PNP^- due to the deprotonation of the hydroxy group. However, the anionic form PNP^- prevailed when the pH > 9.

The interaction between PNP and AC was very complicated according to the forms of PNP and surface charge of the AC at different pH (Fig. 9). There are a large number of carbonyl functional group(-COOH) and hydroxyl functional groups(-OH) on surface of AC which was observed from the FTIR spectra of AC in Fig. 3. At pH < 6, PNP^0 adsorption was mainly via π-π interaction between the π-electrons in a carbonaceous adsorbent and the π-electron in the aromatic ring of PNP[24,25] and H-bonding between the hydroxyl group of PNP molecule and the carbonyl groups on adsorbent surface in acidic solutions.[12] When the initial pH value exceeded 6, H-bonding will be weakened due to the deprotonation of the hydroxy group, leading to the weak decrease of PNP adsorption capacity. At pH > pH_{pzc}, the surface charge of the AC is negative. Meanwhile, PNP began to dissociate and existed as anions. Thus, the negative charges on the adsorbent surface would result in electrostatic repel for PNP^-,[23] and the PNP only adsorbed on adsorbent by π-π interaction. As a result, the adsorption amount sharply decreased at basic pH.

Kinetics study

The adsorption kinetics of PNP adsorbed on AC was study. In order to determinate the mechanism of PNP adsorbed on AC, several adsorption kinetics models were applied. The kinetic models are displayed in Figs. 10-13, and kinetics parameters were shown in Table 1.

As seen from the Table 1, it is clearly that the values of q_{exp} agreed with the values calculated from the nolinear plots of the pseudo-first-order kinetic model, and the values of R^2 were higher than 0.97. For the pseudo-second-order kinetic model, the values of R^2 were higher than 0.97, but the values of q_{cal} failed to match the q_{exp}. It is clearly that pseudo-first-order model gives a satisfactory fit to all of the experimental data. Due to the low R^2, the Elovich model can't describe the adsorption of PNP onto AC.

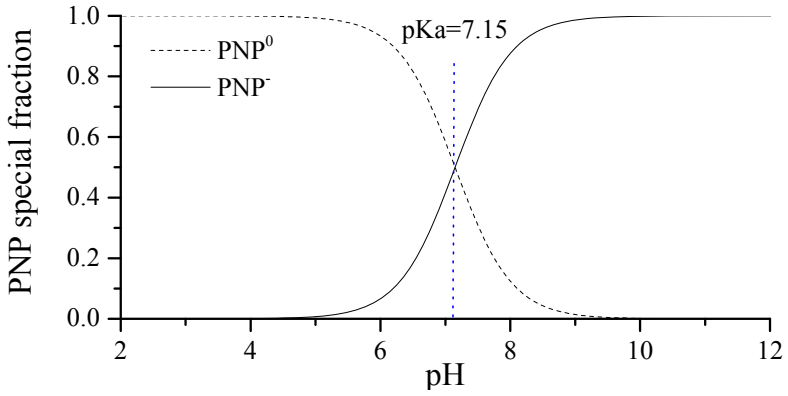

Fig. 8 – The distribution coefficient of PNP.

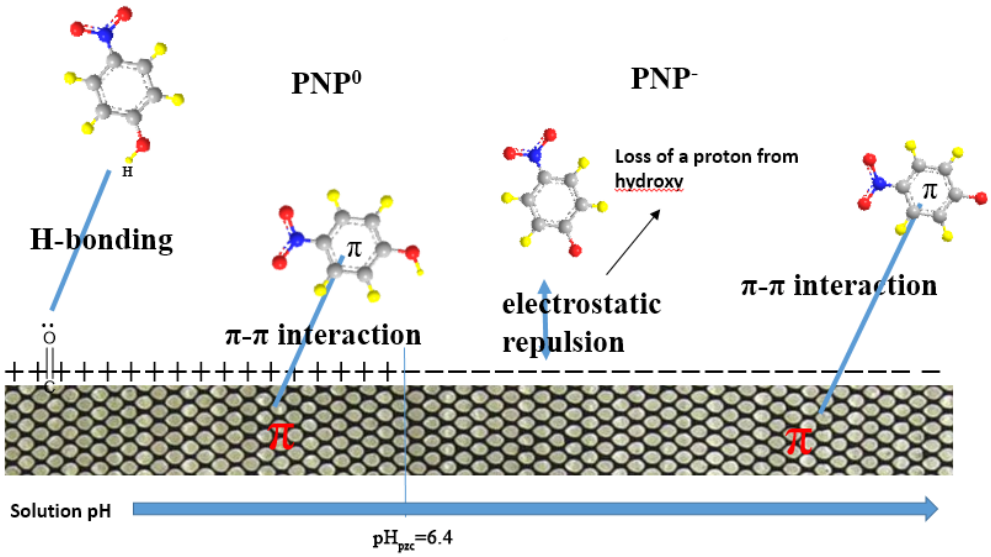

Fig. 9 – The contact model of PNP adsorption on AC at different pH.

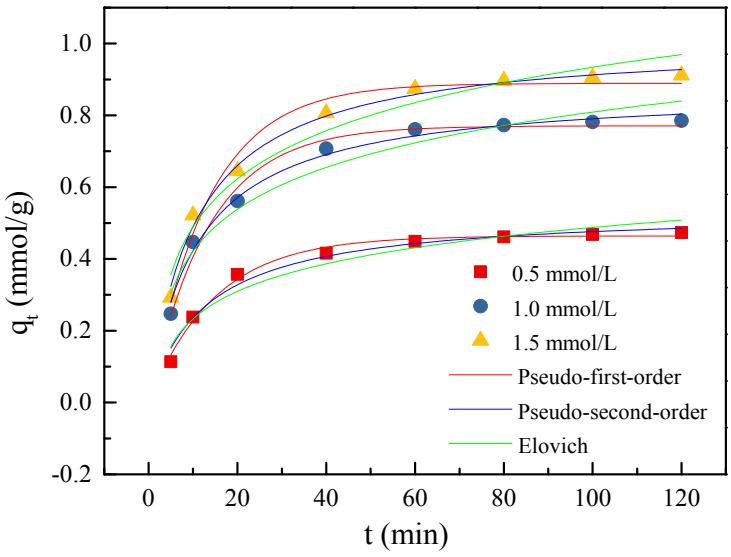

Fig. 10 – Kinetic models at different initial *p*-nitrophenol concentrations.

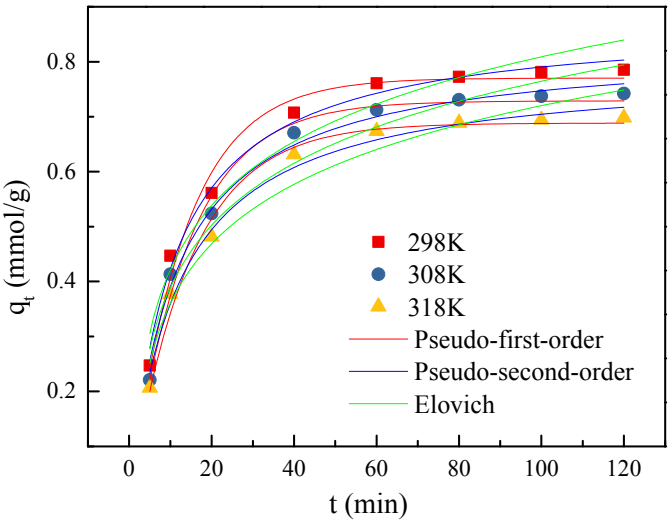

Fig. 11 – Kinetic models at different temperature.

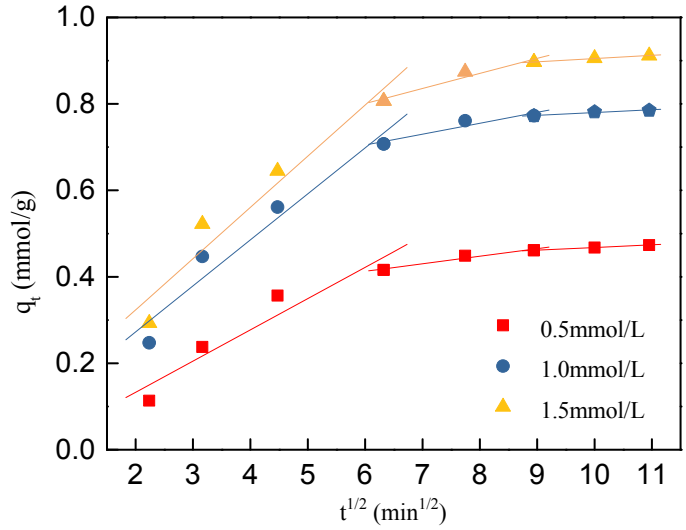

Fig. 12 – Intra-particle diffusion model at different initial concentrations.

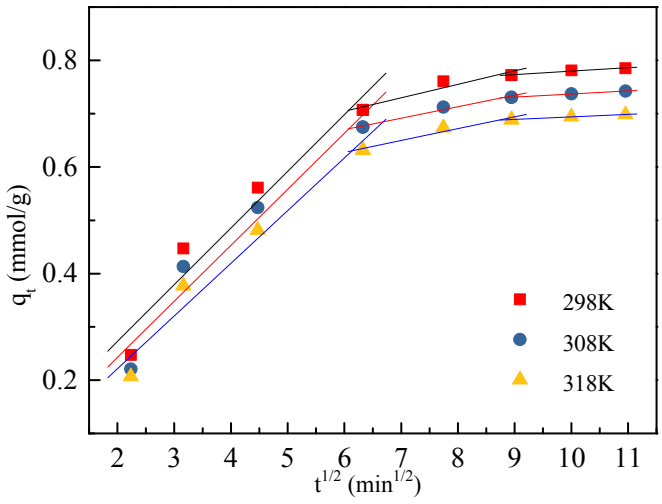

Fig. 13 – Intra-particle diffusion model at different temperature.

Fig. 12 and Fig. 13 show the linear fit of the intra-particle diffusion model for the PNP adsorption process. The parameters calculated were listed in Table 1. The intra-particle diffusion model had three steps, indicating that more than one process can affected the PNP adsorption. The first stage was a quick external surface adsorption and probably attributed to the diffusion of PNP through the solution to the external surface of AC or the boundary layer diffusion of solute molecules. The second step was a gradual adsorption stage for which the intra-particle diffusion rate is rate-limiting. The end step was a final equilibrium stage. It was clear that none of the lines pass through the origin, suggesting that the intra-particle diffusion is not the only rate-controlling step, other mechanisms such as boundary layer may affect the PNP adsorption process.

Table 1

Kinetic parameters of *p*-nitrophenol adsorption onto the activated carbon

C_0/T	0.5 mmol/L	1.0 mmol/L	1.5 mmol/L	298K	308K	318K
Pseudo-first-order model						
k_1 (1/min)	0.0674	0.0750	0.0754	0.0750	0.0720	0.0687
q_{cal} (mmol/g)	0.46	0.77	0.89	0.77	0.73	0.69
q_{exp} (mmol/g)	0.47	0.78	0.91	0.78	0.74	0.70
R^2	0.9893	0.9828	0.9758	0.9828	0.9855	0.9869
Pseudo second-order model						
k_2(g/mmol min)	0.1465	0.1072	0.0937	0.1072	0.1066	0.1065
q_{cal} (mmol/g)	0.54	0.88	1.00	0.87	0.83	0.79
R^2	0.9750	0.9886	0.9908	0.9886	0.9872	0.9879
Elovich kinetic						
α	0.0910	0.2063	0.2432	0.2063	0.1779	0.1569
β	9.0426	5.9457	5.1784	5.9458	6.1388	6.4018
R^2	0.9339	0.9473	0.9560	0.9473	0.9474	0.9516
Intra-particle diffusion model						
k_{t1} (mmol/g $min^{1/2}$)	0.1063	0.1051	0.0988	0.0722	0.1063	0.1183
C_1	0.0602	0.0329	0.0240	0.0113	0.0602	0.0877
R^2	0.9430	0.9502	0.9618	0.9128	0.9430	0.9376
k_{t2} (mmol/g $min^{1/2}$)	0.0253	0.0231	0.0222	0.0176	0.0253	0.0348
C_2	0.5530	0.5279	0.4948	0.3070	0.5530	0.5924
R^2	0.9095	0.9712	0.9526	0.9600	0.9095	0.9479

Table 1 (continued)

k_{t3} (mmol/g min$^{1/2}$)	0.0064	0.0058	0.0047	0.0061	0.0064	0.0074
C_3	0.7156	0.6794	0.6472	0.4072	0.7156	0.8301
R^2	0.9639	0.9982	0.9934	0.9980	0.9626	0.9934

Adsorption isotherms

The interaction between the PNP and AC was investigated via the adsorption isotherms. The difference between the experimental data and each model can be verified by the chi-square.[26] There, non-linear chi-square statistical test was given as:

$$\chi^2 = \sum \frac{\left(q_{e,exp} - q_{e,cal}\right)^2}{q_{e,\exp}} \qquad (10)$$

where $q_{e,exp}$ and $q_{e,cal}$ are the experimental and calculated adsorption uptakes, respectively.

Fig.14 indicates the adsorption isotherm models of PNP on AC at different temperature. The parameters of isotherm models were given in Table 2. The values of R^2 obtained from Langmuir equation were higher than 0.978, and the values of χ^2 were lower than 0.02, indicating that Langmuir model can well describe the PNP adsorption process. And the maximum monolayer adsorption capacities of AC for PNP were found to be 1.03 mmol/g, 0.99 mmol/g, and 0.96 mmol/g at 298, 308 and 318 K, respectively. Higher value of K_L indicates PNP adsorption on AC was a favorable process. With the temperature from 298 to 318 K, the values of K_L decreased from 7.3325 to 7.1381, which also suggested that the higher temperature is negative for adsorption. So the adsorption process may be an exothermic process.

The Freundlich parameter $1/n$ relates to the surface heterogeneity. From the Table 2, $1/n$ is higher than 0 but lower than 1, which indicated that the PNP adsorption behavior was carried out easily.

R^2 obtained from Temkin model are all higher than 0.96. But it was observed that with the temperature increasing from 298 to 318 K, the change of a_t had no law. The Temkin model cannot describe the PNP adsorption process.

As for Redlich-Peterson isotherm model, the values of g were all more than 1, indicating that the Redlich-Peterson isotherm was not the reasonable model to describe the PNP adsorption process.

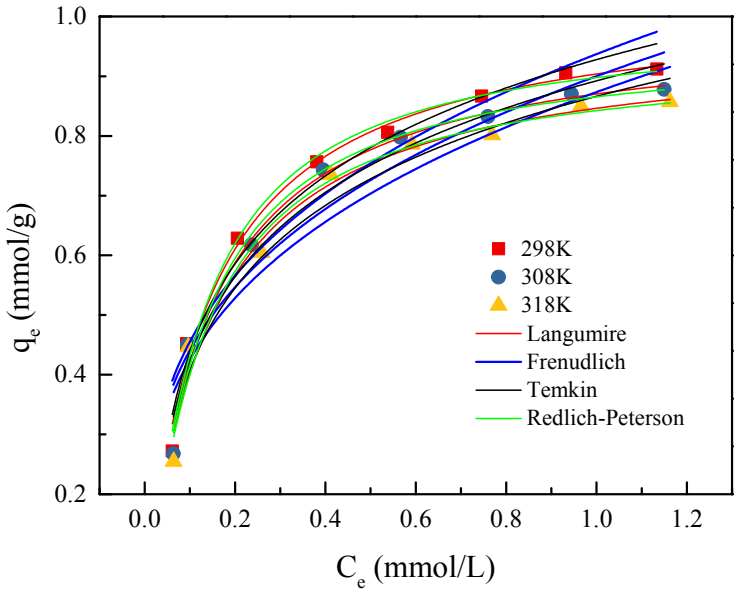

Fig. 14 – The isotherm models at different temperature.

Table 2

Parameters of adsorption isotherm

Parameters	298 K	308 K	318 K
Langmuir isotherm			
q_m	1.03	0.99	0.96
K_L	7.3325	7.3072	7.1381
R^2	0.9884	0.9852	0.9781
χ^2	0.01	0.01	0.02
Freundlich isotherm			
K_F	0.9371	0.9001	0.8735
$1/n$	0.3132	0.3098	0.3123
R^2	0.9174	0.9121	0.9075
χ^2	0.06	0.06	0.07
Temkin isotherm			
a_t	78.7112	79.5583	77.0097
b_t	11.6574	12.5594	13.2561
R^2	0.9720	0.9670	0.9616
χ^2	0.02	0.02	0.03
Redlich-Peterson isotherm			
A	7.1853	6.8487	6.6153
B	6.9769	6.8972	6.8366
g	1.0237	1.0270	1.0199
R^2	0.9864	0.6982	0.9739
χ^2	0.01	0.01	0.02

Table 3

Comparison of PNP adsorption capacities of AC produced by low-cost material

Adsorbent	Adsorption capacities	References
Activated carbon from carrot dross	125 mg/g	TR Bastami *et al.*[27]
Activated carbon prepared from coal tar pitch and furfural	132 mg/g	H Altaher *et al.*[28]
Activated carbon prepared from date pits	108.7 mg/g	MA Al-Ghouti *et al.*[29]
Activated carbon prepared from the lignin	1.03 mmol/g(142.87 mg/g)	This work

The comparison of maximum monolayer adsorption capacity of the AC (this work) for PNP removal with the activated carbon produced by some other low-cost materials is shown in Table 3. Result shows that the AC prepared from lignin of cellulosic ethanol by-product had a relatively large PNP adsorption capacity and can be considered as a promising adsorbent for the removal of PNP.

CONCLUSION

The adsorption characteristics of PNP onto AC derived from lignin of cellulosic ethanol by-product were investigated. The Langmuir isotherm was the best model to describe the PNP adsorption process. The maximum monolayer adsorption capacity of AC was 1.03 mmol/g at 298 K. The kinetic calculations showed that the adsorption data fitted the pseudo-first-order model well, indicating that the PNP adsorption on AC was an physical absorption process. As for intraparticle diffusion model, it was clear that PNP adsorption process was not only controlled by the intra-particle diffusion, boundary layer may affect the adsorption process in some way. The H-bonding, π-π interaction and electrostatic repulsion were suggested to be involved in the PNP adsorption process. AC derived from lignin of cellulosic ethanol by-product was the promising material for the removal of PNP due to its large adsorption capacity and low-cost.

Acknowledgements: Thanks of authors are extended to Science and Technology Department of Henan Province (Grant No.162102210002) and the Education Department of Henan Province in China (Grant No.14A530005) for the financial support of this study.

REFERENCES

1. C. Solisio and B. Aliakbarian, *Can. J. Chem. Eng.*, **2017**, *95*, 1760-1767.
2. W. Liu, J. Zhang, C. Zhang and R. Liang, *Chem. Eng. J.*, **2011**, *171*, 431-438.
3. G. Xue, M. Gao, Z. Gu, Z. Luo and Z. Hu, *Chem. Eng. J.*, **2013**, *218*, 223-231.

4. D. Tang, Z. Zheng, K. Lin, J. Luan and J. Zhang, *J. Hazard. Mater*., **2007**, *143*, 49-56.
5. J. Zhou, Z. Zhang, B. Cheng and J. Yu, *Chem. Eng*. *J*., **2012**, *211-212*, 153-160.
6. P. T. Huong, B. K. Lee and J. Kim, *Process Saf. Environ*., **2016**, *104*, 314-322.
7. O. Gimeno, M. Carbajo, F. J. Beltrán and F. J. Rivas, *J. Hazard. Mater*., **2005**, *119*, 99-108.
8. M. Ksibi, A. Zemzemi and R. Boukchina, *J. Photoch Photobio A*., **2003**, *159*, 61-70.
9. S. W. Peretti, C. J. Tompkins, J. L. Goodall and, A. S. Michaels, *J. Membrane Sci*., **2002**, *195*, 193-202.
10. M. Z. Khan, P. K. Mondal and S. Sabir, *Can. J. Chem.Eng*., **2013**, *91*, 1045-1058.
11. B. Zhang, F. Li, T. Wu, D. Sun and Y. Li, *Colloid Surface A*., **2015**, *464*, 78-88.
12. M. Erdem, E. Yüksel, T. Tay, Y. Cimen and H. Türk, *J. Colloid Interf SCI*., **2009**, *333*, 40-48.
13. O. Layaly, E. K. Nadia, T. Delphine, W. Mathias and B. Agnès, *J. Colloid Interf SCI*., **2015**, *457*,218-224.
14. B. Petrova, T. Budinova, B. Tsyntsarski, V. Kochkodan, Z. Shkavro and N. Petrov, *Chem. Eng. J*., **2010**, *165*, 258-264.
15. X. L. Han, Y. Y. He, H. H. Zhao and D. Wang, *Korean J. Chem. Eng*., **2014**, *31*, 1810-1817.
16. W. O. S. Doherty, P. Mousavioun and C. M. Fellows, *Ind. Crop. Prod*., **2011**, *33*, 259-76.
17. G. Liu and J. Bao, *Bioresour. Technol*., **2017**, *243*, 1232-1236.
18. M. Martin-Martinez, M. F. F. Barreiro, A. M. T. Silva, J. L. Figueiredo, J. L. Faria and H. T. Gomes, *Appl. Catal. B-Environ*., **2017**, *219*, 72-378.
19. S. Román, J. F. González, C. M. González-García and F. Zamora, *Fuel. Process. Technol*., **2008**, *89*,715-720.
20. J. Rivera-Utrilla, I. Bautista-Toledo, M. A. Ferro-García and C. Moreno-Castilla, *J. Chem. Technol. Biotechnol*., **2001**, *76*, 1209-1215.
21. Y. Park, R. L. Frost, G. A. Ayoko and D. L. Morgan, *J. Therm. Anal. Calorim*., 2013,*111*,41–47.
22. B. P. Zhang, X. L. Han, P. G. Gu, S. Q. Fang and J. Bai, *J. Mol. Liq*., 2017,*238*,316-325.
23. L. M. Cotorueloa, M. D. Marquesa, F. J. Diaza, J. Rodriguez-Mirasola, J. J. Rodriguezb and T. Corderoa, *Chem. Eng. J*., **2012**, *184*, 176-183.
24. J. H. Chen, X. Sun, L. J. Lin, X. F. Dong and Y. S. He, *Chin. J. Chem. Eng*., 2017, *25*, 775-781.
25. H. S. Zheng, W. Q. Guo, S. Li, Y. D. Chen, Q. L. Wu, X. C. Feng, R. L. Yin, S. H. Ho, N. Q. Ren and J. S. Chang, *Bioresour. Technol*., **2017**, *244*, 1456-1464.
26. M. Ghaedi, B. Sadeghian, A. A. Pebdani, R. Sahraei, A. Daneshfar and C. Duran, *Chem. Eng. J*., **2012**, *187*, 133-141.
27. T. R. Bastami and M. H. Entezari, *Chem. Eng. J*., **2012**, *210*, 510-519.
28. H. Altaher and A. M. Dietrich, *Water Sci. Technol*., **2014**, *69*, 31-37.
29. M. A. Al-Ghouti, M. A. Khraisheh, S. J. Allen and M. N. Ahmad, *J. Environ. Manage.*, **2003**, *69*, 229-238.